Geojournal of Tourism and Geosites
ISSN 2065-0817, E-ISSN 2065-1198

Year XVIII, vol. 63, no. 4spl, 2025, p.2788-2799
DOI 10.30892/gtg.634spl23-1638

INTEGRATED UAV, GNSS AND GPR METHODS FOR KARST TERRAIN ANALYSIS IN AN ARID REGION: A CASE STUDY FROM THE SAURA VALLEY, WESTERN KAZAKHSTAN

Aruzhan BEKTURSYNOVA [1*], Roza TEMIRBAYEVA [1], Yuisya LYY [1], Zhanerke SHARAPKHANOVA [1]

[1] Institute of Geography and Water Security - JSC, Laboratory of Geotourism and Geomorphology, Almaty, Kazakhstan; aru.bekkuliyeva@gmail.com (A.B.); temirbayr@gmail.com (R.T.); uisya_lyi77@mail.ru (Yu.L.); sharaphanova@gmail.com (Zh.Sh.)

Citation: Bektursynova, A., Temirbayeva, R., Lyy, Yu., & Sharapkhanova, Zh. (2025). Integrated UAV, GNSS and GPR methods for karst terrain analysis in an arid region: A case study from the Saura valley, western Kazakhstan. *Geojournal of Tourism and Geosites*, 63(4spl), 2788–2799. https://doi.org/10.30892/gtg.634spl23-1638

Abstract: Karst processes have a significant impact on the formation of the relief in the Mangystau region (Western Kazakhstan), where arid climatic conditions and the predominance of carbonate rocks contribute to the development of both surface and subsurface karst forms. The aim of this study is the identification of potential geohazards in the Saura Valley (Mangystau region) through an integrated surface and subsurface investigation method. The methodological framework combines high-resolution photogrammetry using an unmanned aerial vehicle (UAV), GNSS georeferencing, and low-frequency ground-penetrating radar profiling. UAV surveys with the Autel EVO II RTK Pro (V3) produced orthophotomaps and a digital elevation model (DEM), which formed the basis for detailed morphometric analysis. Subsurface investigations using the GPR Zond Aero LF identified three distinct loosening zones that coincided with structural faults. GNSS measurements with the SOUTH Galaxy G9 receiver ensured centimeter-level spatial accuracy across all datasets. The collected data were integrated and analyzed within a GIS environment to establish spatial correlations between surface morphology, geophysical anomalies, and tectonic structures. The results confirm the structurally controlled nature of karst development and demonstrate the effectiveness of an integrated approach for detecting potentially unstable karst zones in arid environments. Geotourism represents a promising direction for the rational use of karst terrains, offering scientific, aesthetic, and recreational benefits. However, the environmental vulnerability of karst terrains requires a balanced approach to tourism development, incorporating long-term monitoring and planning to preserve their natural integrity.

Keywords: Karst terrain, arid regions, morphometric analysis, lineaments, Saura Valley

* * * * * *

INTRODUCTION

Karst landscapes are the result of long-term chemical weathering and dissolution of soluble rocks, such as carbonates (limestones, dolomites) and evaporites, leading to distinctive surface and subsurface features including sinkholes, dolines, caves, and karst valleys. The dominance of dissolution processes over mechanical erosion gives rise to complex morphologies and hydrological dynamics that pose significant geohazards, particularly in regions affected by structural deformation and groundwater flow variability (Gutiérrez et al., 2014; Potapova & Bekkuliyeva, 2010a).

In recent years, there has been growing international interest in applying high-resolution remote sensing and geophysical methods to the analysis of karst terrain. UAV-based photogrammetry, GNSS positioning, and ground-penetrating radar (GPR) are increasingly used to detect, map, and characterize karst landforms and subsurface voids with high spatial accuracy (Gutiérrez et al., 2011; Siart et al., 2009; El Hameedy et al., 2023; Ebraheem & Ibrahim, 2019; Moslemi et al., 2023). These technologies have proven particularly effective in humid and temperate regions (Diercks et al., 2023; Tallini, 2006; La Salandra, 2022; Öztürk et al., 2025), yet their application in Central Asian arid karst systems remains limited. Arid environments introduce specific challenges for karst development and detection, including low precipitation, sparse vegetation, and limited surface water, which often mask subsurface instability (Large & Heritage, 2009; Al-Rawabdeh et al., 2016; Theilen-Willige et al., 2014).

The Mangystau region in western Kazakhstan is one such arid zone, characterized by a unique geological setting dominated by fractured Neogene limestones and marl interlayers. Despite evidence of extensive karst formation, including sinkholes, collapsed depressions, and shallow caves, the region remains understudied using modern geospatial and geophysical techniques. Most prior investigations, particularly those conducted during Soviet-era geological surveys, lacked the resolution and precision required to fully assess karst morphometry or subsurface structure (Potapova & Bekkuliyeva, 2010b; Iskakov, 2019; Aliyev, 2015). The first specialized work on the karst of Ustirt and Mangystau was authored by geomorphologist Yu.Ya. Kuznetsov, who highlighted the wide development of surface and underground karst

* Corresponding author

formations in the desert region (Kuznetsov, 1965). The Saura valley in the Mangystau region provides an optimal setting for advanced karst investigations, characterized by pronounced surface deformation, steep erosional slopes, and a partially water-filled depression indicative of active subsurface karstification. Beyond its geomorphological importance, the site attracts increasing numbers of tourists, raising concerns about slope stability and public safety. These conditions make Saura a representative case study for assessing geohazards in arid karst environments.

The karst processes observed in the Saura valley show significant similarities with karst systems in arid regions of other countries. Comparative analysis suggests that the karst valley Saura has a number of common geological and hydrological characteristics with western Iran and Saudi Arabia. The study by Ghadimi et al., emphasizes that karst formation in western Iran is associated with seasonal moisture, mainly due to snowmelt and episodic rainfall, which is also typical for the conditions of Saura (Ghadimi et al., 2022). A similar situation is observed in Saudi Arabia, where karst forms develop in a hyper-arid climate. According to Youssef et al., the presence of easily soluble rocks (carbonates and evaporites) in combination with natural and anthropogenic factors leads to the widespread occurrence of sinkholes and soil instability (Youssef et al., 2016).

Karst terrains represent one of the most challenging environments for engineering, mining, and construction activities due to their highly heterogeneous subsurface structures. The presence of cavities, sinkholes, and dissolution zones often leads to severe geotechnical hazards, including ground subsidence and structural failure. Therefore, the application of advanced geophysical methods plays a crucial role in improving the reliability of karst mapping and in mitigating risks associated with subsurface instability. Among these methods, Ground Penetrating Radar (GPR) has proven to be particularly effective for detecting near-surface structural anomalies that may otherwise remain undetected.

The ability of GPR to provide high-resolution imaging makes it valuable not only for mapping subsurface cavities but also for supporting accident prevention (Yalcin, 2025). In the context of risk assessment and monitoring of karst areas in arid zones, the use of remote sensing methods seems relevant. In the study of Aigner et al., detailed mapping of sinkholes in arid areas of the Mangystau region (Kazakhstan) was carried out using open satellite data. Geospatial analysis revealed spatial relationships between karst sinkholes, takyrs, vegetation cover and potential surface runoff, which opens up new opportunities for early diagnosis of karst risks in conditions of limited water supply (Aigner et al., 2025).

The aim of this study is identification of potential geohazards in the Saura Valley (Mangystau region) through an integrated surface and subsurface investigation methods. We used UAV-based digital elevation modeling, GNSS ground control, and low-frequency GPR profiling to: Generate a detailed DEM; Detect zones of subsurface soil loosening and void development; Analyze the spatial correlation between geomorphic features and structural lineaments. The integrated use of UAV, GNSS, and GPR technologies enables accurate identification and spatial analysis of karst-related features in arid landscapes, offering significant advantages for geohazard assessment and long-term monitoring in data-scarce regions.

STUDY AREA

The study was conducted in the Saura Valley, located in the northwestern part of the Mangystau region of western Kazakhstan. This region lies within an arid climatic zone between the Caspian and Aral Seas and is characterized by predominantly desert landscapes. The Saura Valley is situated approximately 90 km northeast of the city of Aktau and represents a distinct karst-erosional depression within a geologically and geomorphologically complex setting (Figure 1). Due to its unique geological formations, nature contrast, and relative accessibility from the city of Aktau, the Saura has become a popular destination for domestic and international tourists, including hikers, and nature photographers.

The valley exhibits a semi-circular planform bounded by steep escarpments and is defined by a range of surface karst features, including sinkholes, collapsed blocks, and erosional scarps. Particularly on the right slope of the valley, debris flow and landslide processes are active, with individual rock fragments reaching up to 5 meters in diameter. These features indicate ongoing gravitational instability exacerbated by lithological variability and precipitation events.

Figure 1. Overview map of the study area

A key geomorphic element within the valley is the Saura Grotto, a horseshoe-shaped karst sinkhole partially filled with water (Aliyev, 2015) (Figure 2). Its vertical walls reveal distinct horizontal stratification, consistent with the sedimentary origin of the host limestones (Kulbayeva, 2018). The persistent presence of water and moisture-loving vegetation around the depression margins suggests ongoing groundwater emergence and localized infiltration processes.

Figure 2. Saura Valley (Source: Photo taken by employees of the laboratory of Geotourism and geomorphology of the "Institute of Geography and Water Security" JCS, 06.05.2025)

Geologically, the area is composed predominantly of Neogene-age carbonate rocks, including limestones and marl interlayers, with widespread fracturing and thin Quaternary cover (Gvozdetczky, 1972; Nechayev & Strokova, 2023; Kuznetsov, 1965; Kleiner, 1970). The site lies within a structural transition zone where platform-type tectonic blocks intersect folded belts, creating fracture networks that promote subsurface water circulation (Tsirélson & Popov, 2010). These structural conditions are favorable for both surface and subsurface karst development. Multiple phases of uplift and denudation from the Neogene to Quaternary periods have further enhanced karstification by exposing carbonate strata to water infiltration (Chikishev, 1973; Vlasov, 1988; Ford & Williams, 2007; Goldscheider & Drew, 2007; Akziz et al., 2022).

From a geomorphological perspective, the valley is positioned at the boundary between an abrasion-accumulative marine terrace and a structurally armored plateau surface. This transitional setting contributes to surface runoff concentration and vertical moisture migration through fractured rock layers (Le Mesnil et al., 2021).

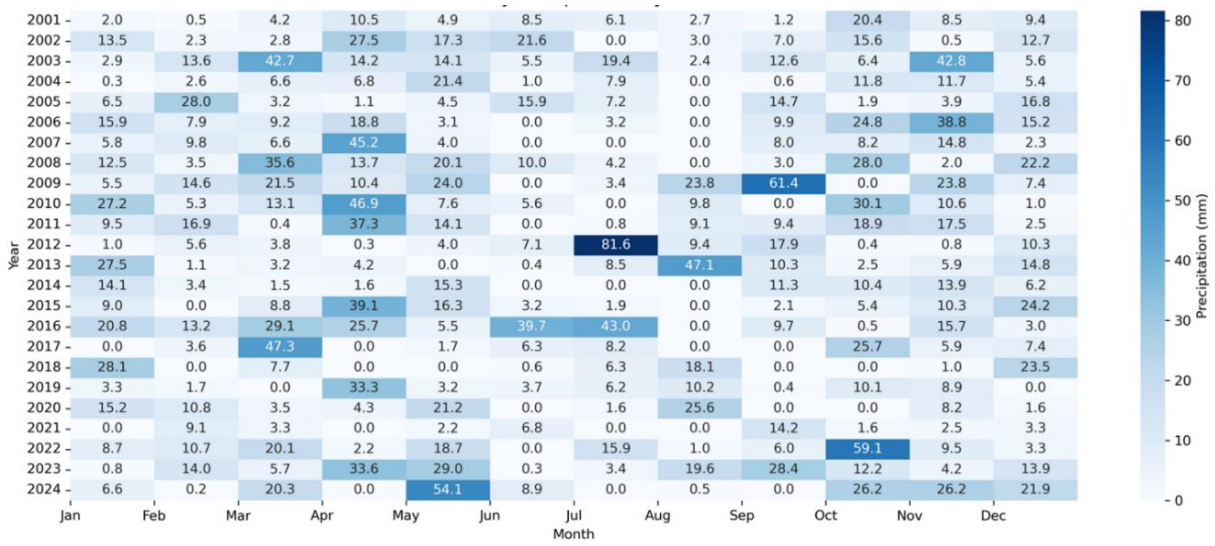

Figure 3. Monthly Precipitation by Year (Source: https://kazhydromet.kz)

The landscape is dominated by shallow depressions, cliffs, collapsed zones, and disrupted morphostructures features typical of karst systems in arid regions with minimal surface drainage (Torsuyev, 1980). Climatically, the region

experiences a desert-continental regime with average annual temperatures of 11.5–12 °C. Seasonal extremes range from –37 °C in winter to +42 °C in summer. Annual precipitation averages 130–170 mm, with peak values occurring in spring (particularly April) (http://ecodata.kz) (Figure 3). Despite the low total precipitation, episodic snowmelt and storm events generate highly aggressive infiltration, contributing to the chemical weathering of exposed carbonates. The area also experiences persistent wind activity exceeding 5 m/s, predominantly from the east and southeast (https://kazhydromet.kz).

The local soil and vegetation conditions further reflect karst-related hydrological dynamics. Moisture-loving species are concentrated in zones of groundwater emergence and seepage, while brown solonetzic and non-solonetzic soils dominate across the valley floor and slopes. These edaphic variations serve as indicators of subsurface water pathways and infiltration intensity. Due to the presence of well-developed karst landforms, extensively fractured carbonate lithology, seasonally variable hydrological conditions, the Saura Valley constitutes an optimal arid-zone karst systems in Mangystau, it offers a unique opportunity to investigate geomorphic evolution, assess terrain stability, and identify potential geohazards within a structurally complex and environmentally sensitive karst landscape. The increasing number of visitors highlights the need for detailed geomorphological and geohazard assessments, especially considering the presence of unstable slopes, rockfalls, and potential subsidence zones. Despite its popularity, the area remains insufficiently studied using modern, high-resolution techniques that could inform risk management and sustainable tourism development.

MATERIALS AND METHODS

A comprehensive field investigation of the Saura Valley was conducted using an integrated methodology, combining archival research, UAV-based (Unmanned Aerial Vehicle) photogrammetry, GNSS (Global Navigation Satellite System) surveying, and GPR (ground-penetrating radar) profiling. This multi-method approach enabled both surface and subsurface characterisation of the karst landscape.

Prior to fieldwork, a literature review was conducted to examine the geological, geomorphological, and hydrogeological context of the study area. The analysis revealed a lack of prior high-resolution studies focused specifically on the Saura Valley.

1. GNSS Surveying and Data Integration

High-precision georeferencing was achieved using the SOUTH Galaxy G9 GNSS receiver, which supports multi-frequency and multi-constellation tracking. Its integrated RTK functionality and 4G modem provided real-time kinematic corrections, ensuring centimetre-level accuracy. GNSS data were used not only for positioning UAV imagery and GPR profiles, but also for constructing spatial base layers in GIS (Geographic Information System).

2. UAV-Based Photogrammetry

UAV-based photogrammetry is an increasingly adopted technique in karst terrain analysis, offering cost-effective, high-resolution data acquisition in areas where satellite imagery is limited or unavailable (Prodanov et al., 2019; Vassilakis & Konsolaki, 2022). High-resolution aerial surveys were carried out using the Autel EVO II RTK Pro (V3) UAV. This drone is characterized by the following technical parameters: 6K resolution camera with a 1-inch CMOS sensor (20 MP), 29 mm equivalent lens, adjustable aperture from f/2.8 to f/11. The RTK module provides centimetre-level positioning accuracy for high-precision photogrammetric data acquisition (https://www.autelrobotics.com). The UAV survey covered an area of 70 582 m^2. The flight was performed in autonomous mode, with the route preloaded into the drone controller. The drone was launched to an altitude of 120 m at an average speed of approximately 8 m/s; longitudinal and transverse image overlap was maintained at 80%, and the camera angle was set to 90^0. The UAV flight area was selected within the most frequently visited zone, where the majority of tourist activity is concentrated.

Ground control points were pre-marked and measured using the SOUTH Galaxy G9 GNSS receiver, with horizontal and vertical accuracy of 1-2 cm, referenced to UTM Zone 39N. Photogrammetric processing was conducted in Agisoft Metashape using Structure-from-Motion (SfM) techniques (Garova et al., 2025; Westoby et al., 2012; Jarzyna et al., 2024). The workflow included photo alignment, dense point cloud generation, mesh reconstruction, and texture mapping. Ground control points were manually identified and assigned GPS (Global Positioning System) coordinates with elevation values. The resulting orthophoto and digital elevation model (DEM) were exported and further analysed in ArcGIS.

3. Ground-Penetrating Radar (GPR) Survey

Karst cavities, often lacking direct surface access, are well-suited for investigation using non-invasive geophysical techniques. GPR is particularly effective in dry, carbonate terrains due to strong dielectric contrasts between voids and host rock (Funk et al., 2024; Abdeltawab, 2013). GPR is based on the transmission of electromagnetic waves into the subsurface and the recording of reflected waves from objects or interfaces with different dielectric constants. A radar system comprises a signal generator, antennae (for transmission and reception), and a receiver. The system has an onboard computer that facilitates data processing both while acquiring data in the field and post-recording (La Salandra et al., 2022; Takasu & Yasuda, 2009). As the antenna is moved along ground surface, the signals of the reflected waves are displayed as a function of their two-way travel time, i.e. the time elapsed between the transmission and detection by the receiver, in the form of radargram. In low-loss medium the reflection depth of an electromagnetic wave (S) is:

$$S = \frac{t*C}{2\sqrt{\varepsilon_r}} \qquad (1)$$

where t is the two-way travel time, determined from the radargram, C is the speed of light in free space and ε_r is the relative dielectric constant.

The GPR survey was conducted using the Zond Aero LF system. This single-channel, unshielded dipole GPR operates with interchangeable antennas with centre frequencies of 75, 150, and 300 MHz, providing operating bandwidths of 38-150 MHz, 75-300 MHz, and 150-600 MHz (-12 dB), respectively. Data acquisition was performed in real-time sampling mode with hardware stacking, allowing 256 to 8192 samples per scan, a sampling rate of up to 1,280,000 samples s^{-1}, and a scanning speed of up to 2,500 scans s^{-1}. The system records 32-bit digital raw data in standard SEGY (.sgy) geophysical format with geotagged traces. The time range per sample varies from 18 ps to 2.5 ns, enabling a probing depth of up to 12 m in soils with a relative dielectric permittivity of about 5 and a specific attenuation of up to 5 dB m^{-1}. Data processing modes include vertical filtering (off or digital), horizontal filtering (hardware stacking or background removal), and linear gain adjustment from 0 to +168 dB with 1-10 gain points. Raw data are stored with the applied gain parameters, and file size is limited only by the available storage capacity (https://cdn.shopify.com/).

Processing of the radargrams was carried out using Radar Systems Prism2 software. All profiles were subjected to an identical sequence of operations: (i) removal of the background signal; (ii) application of an Ormsby band-pass filter centered on the main frequency with a ±50 % bandwidth; and (iii) adjustment of linear gain to enhance data readability. The reflections marking layer boundaries were then manually identified (Tjoelker et al, 2024).

GPR data acquisition focused on identifying zones of loosening, underground cavities, and subsurface structural heterogeneity. The collected profiles were processed using standard filtering, amplitude correction, and migration techniques to enhance the visibility of anomalies.

4. Post-Processing and Spatial Analysis

In post-fieldwork conditions, the collected datasets were integrated within a GIS framework. A comparative analysis of UAV-derived topographic data, GPR anomalies, and GNSS ground control points was performed to assess spatial correlations between surface morphometric features and subsurface structures. This enabled the identification of zones with increased karst potential and structural instability within the valley.

A particular focus was placed on the detection and interpretation of lineaments, which are linear or curvilinear features often corresponding to geomorphological discontinuities or tectonic structures (El Hadani, 1981). These features may represent fault lines (Faure, 2001), fracture zones, morphological boundaries (Samuel et al., 2010), or zones of mechanical weakness within the Earth's crust (Masoud et al., 2006; Pour et al., 2013; Lacina, 1996; Hobbs, 1912). Lineaments are frequently associated with drainage alignments and lithological contacts, and their presence is often indicative of intense fracturing, brecciation, and enhanced groundwater flow (Strokova et al., 2020).

To extract lineament patterns, the digital elevation model (DEM) was processed to enhance terrain shading and micro-topographic gradients (Abdelouhed et al., 2021). This was achieved by generating four shaded relief raster layers using the Hillshade tool in ArcGIS (https://pro.arcgis.com), applying varying illumination azimuths (0°, 45°, 90°, and 135°) while maintaining constant solar elevation. The use of multi-directional hillshading improved the visibility of subtle linear features, reducing directional bias and enhancing the detection of tectonically influenced geomorphic structures.

RESULTS AND DISCUSSION

The analysis of the Saura Valley was conducted through a comprehensive integration of GNSS-based georeferencing, UAV photogrammetry, morphometric terrain analysis, ground-penetrating radar (GPR) surveys, and digital lineament detection. This section summarizes the key findings obtained from each methodological component.

1. GNSS Survey and Data Georeferencing

High-precision GNSS data were collected using RTK (Real Time Kinematic) and PPK (Post Processing Kinematic) modes to georeference UAV imagery, ground control points (GCPs), and GPR profiles. Five GCPs (Table 1) were distributed evenly across key terrain features and measured with centimetre-level accuracy (horizontal ~2 cm, vertical ~3 cm), thereby enhancing the accuracy of both the DEM and orthophotomap. Geophysical profile coordinates were synchronised with GNSS data, enabling precise spatial alignment of surface and subsurface datasets.

Table 1. Coordinates of the established ground control points in the Saura Valley (Source: SOUTH Galaxy G9 GNSS receiver)

Point Name	True Latitude	True Longitude	Ellipsoid Height
Mark1	44° 13' 54.16" N	50° 48' 15.88" E	-4.836
Mark2	44° 13' 56.14" N	50° 48' 11.91" E	-2.574
Mark3	44° 13' 54.93" N	50° 48' 11.32" E	-12.790
Mark4	44° 13' 54.82" N	50° 48' 9.74" E	-1.498
Mark 5	44° 13' 52.23" N	50° 48' 12.93" E	-3.415

2. UAV Photogrammetry and Data Processing

UAV-based aerial surveys were conducted using the Autel EVO II RTK Pro (V3), flown at 120 meters altitude with 80% forward and lateral image overlap. Photographic centers were post-processed using TEOBOX software, with PPK correction referencing base station data in RINEX format. The flight area covered approximately 70 582 m^2. Number of images – 195.

Photogrammetric processing was carried out in Agisoft Metashape Professional using Structure-from-Motion (SfM) methods (La Salandra et al., 2022; Takasu & Yasuda, 2009; Zhang et al., 2010). This workflow included photo alignment, dense point cloud generation, classification, and DEM and orthophotomap creation. The final data products were exported in GIS-compatible formats for terrain analysis. A summarised flowchart of the described process is shown in Figure 4.

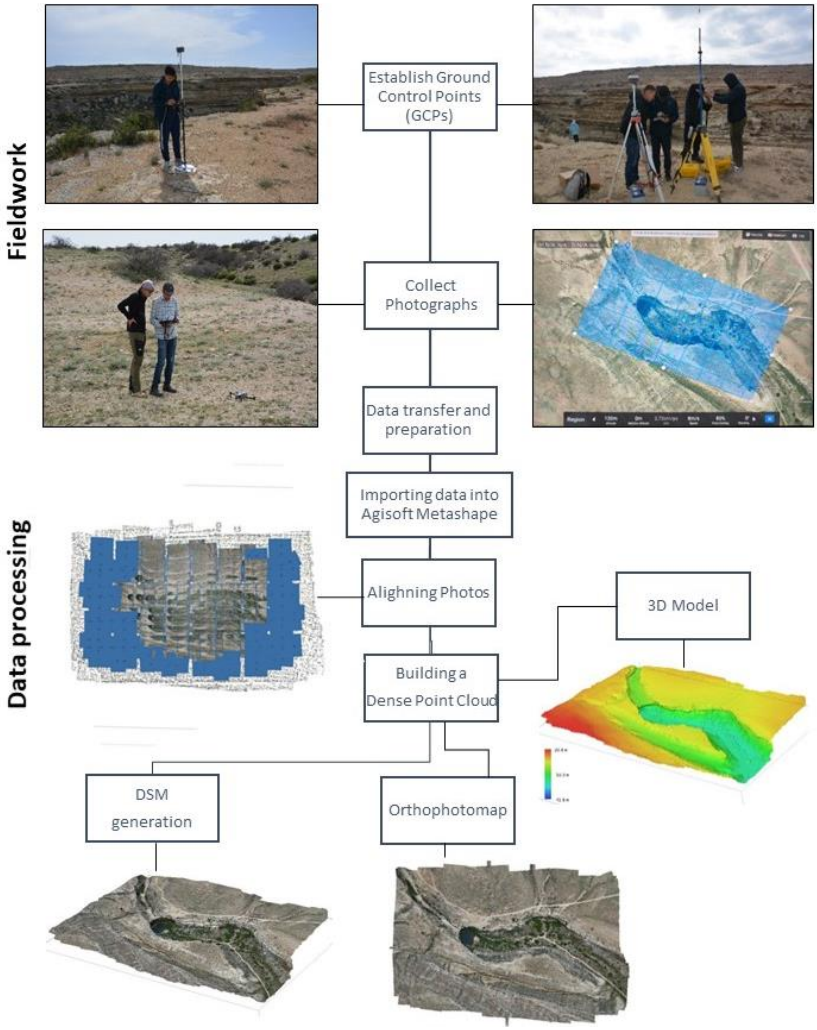

Figure 4. Generalised workflow outline (Source: Prodanov et al., 2019)

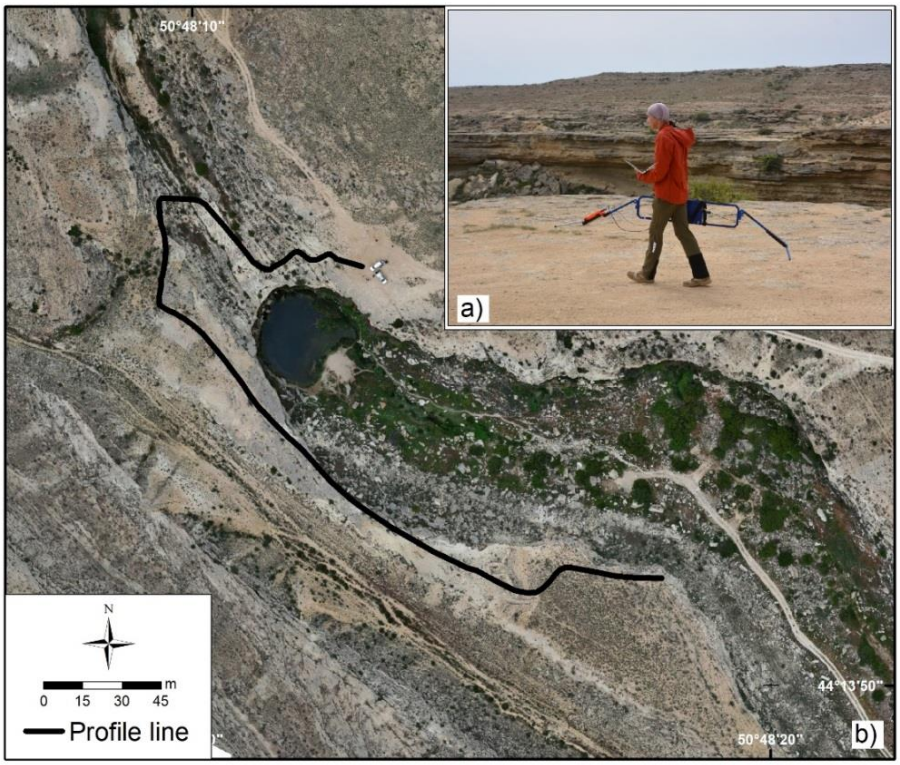

Figure 5. Georadar survey using Zond aero LF 100 MHz (a); Profile diagram of the georadar survey (b). (Source: GPR survey made by Rakhimov & Taskynbayev, 2025)

3. Ground-Penetrating Radar Survey

Subsurface investigations were performed using the Zond Aero LF radar system at 100 MHz (Figure 5). The survey method involved profile-based scanning and data processing in Prism software (Reynolds, 1997). Standard procedures, including background subtraction and gain correction, were applied. Radargrams were interpreted using colour-coded amplitude maps to visualise wave reflections (Frumkin et al., 2011; Batayneh et al., 2002; Tallini et al., 2006; Pueyo-Anchuela et al., 2010; Billi, 2016). In this visualisation, a zero signal amplitude corresponds to a green background on the radargram, positive signal amplitudes are represented by warmer tones progressing to yellow, and negative amplitudes are depicted by cooler tones progressing to blue (Figure 6). Three major zones of subsurface loosening were identified: Zone 1– Adjacent to cliff edges, likely linked to void formation and potential slope failure. Zones 2 and 3 – Possibly associated with water infiltration, filtration flow, or internal erosion. Although GPR anomalies were not yet verified by drilling, their spatial consistency with morphometric and structural indicators supports their interpretation as zones of loosening.

These zones were spatially referenced via GNSS and further visualized in Figure 7.

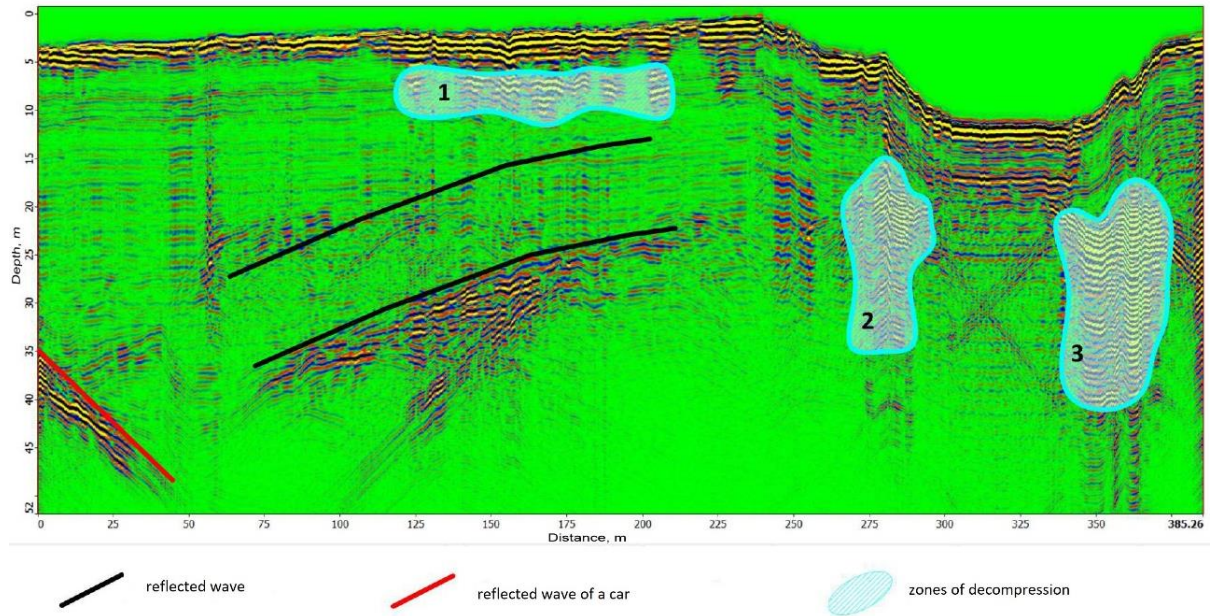

Figure 6. Radar chart with interpretation (Source: interpreted by Rakhimov & Taskynbayev)

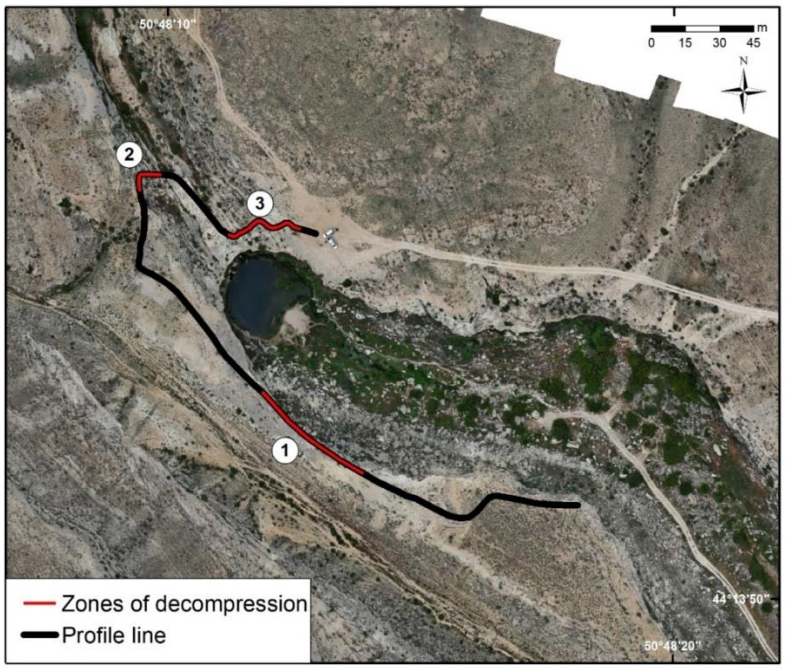

Figure 7. Zones of loosening on the profile diagram (Source: interpreted by Rakhimov& Taskynbayev)

4. Morphometric Terrain Analysis

A DEM generated from UAV imagery was analyzed using ArcGIS Spatial Analyst tools to calculate slope, aspect, curvature, and vertical dissection metrics (Figure 8) (Table 2).

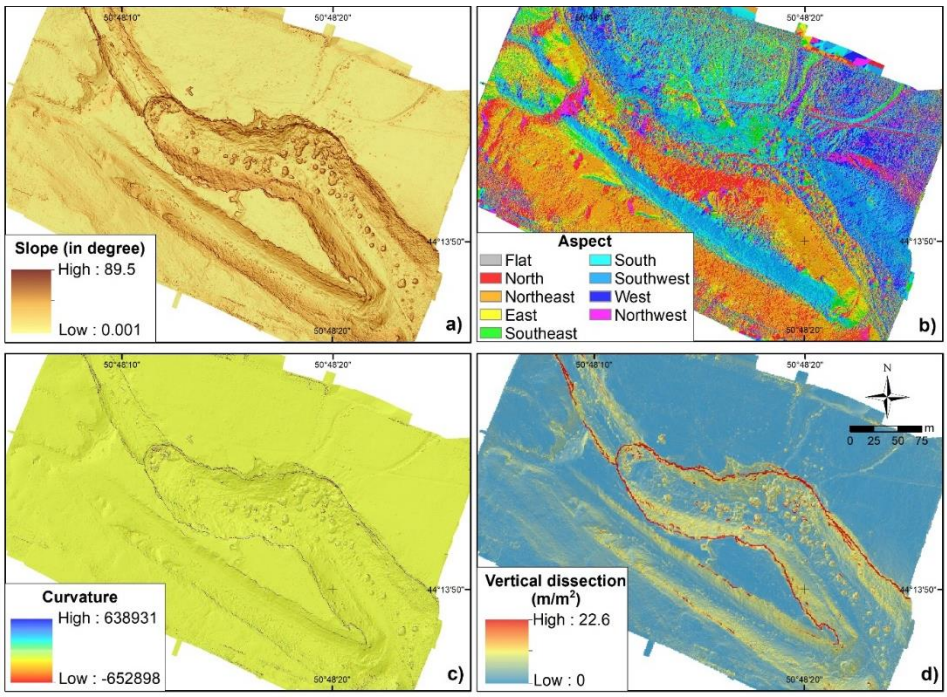

Figure 8. Morphometric characteristics of the terrain in the Saura Valley: a – slope, b – aspect, c – curvature, d – vertical dissection (Source: Based on DEM from UAV, 2025)

Slope ranged from 0.001° to 89.5°, with the steepest areas (>60°) observed along escarpments and rock outcrops. Aspect predominantly faced northeast, southwest, southeast, and south, indicating moisture and vegetation distribution patterns. Curvature values ranged from -652,898 to +638,931, identifying convex and concave terrain forms (https://pro.arcgis.com). Vertical dissection, calculated using Zonal Statistics, reached up to 22.6 m/ml, especially along collapse zones and valley slopes (Pozachenyuk & Petlyukova, 2016; Spiridonov, 1970; Rohaendi et al., 2021; Sharapkhanova et al., 2024).

Table 2. Morphometric characteristics of the Saura Valley and the adjacent area

Morphometric parameters	Min	Max	Mean	St.Dev
Curvature	-652898	638930,6	8,1	3749,5
Slope °	0,001	89,53	14,57	14,28
Vertical Dissection, m/m^2	0	22,6	0,38	0,79

These morphometric parameters provide insights into terrain instability, erosional processes, and moisture flow pathways. Integration with orthophotomaps supports targeted monitoring of geomorphologically hazardous zones.

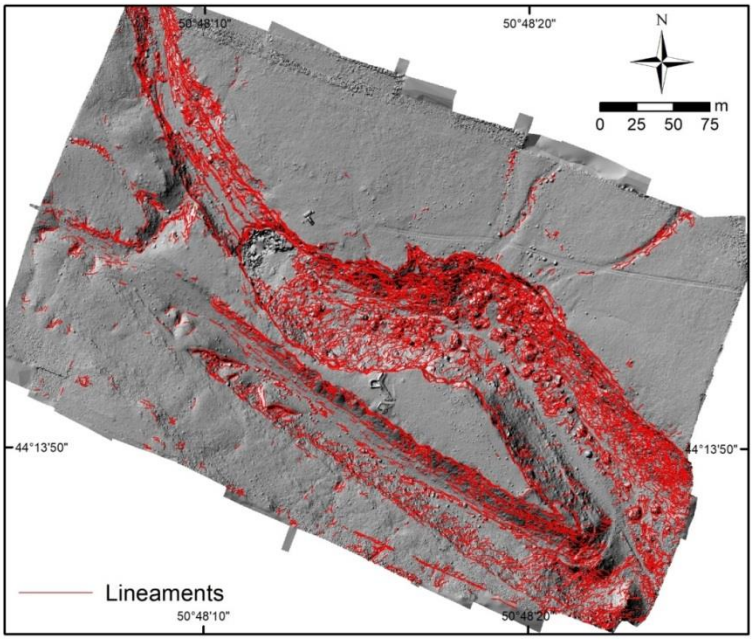

Figure 9. Lineaments obatined in the PCI Geomatica 2018 software (Source: Based on DEM from UAV, 2025)

5. Lineament Detection Using DEM

Lineament analysis was performed to identify tectonic and structural controls on karst development. Shaded relief models were generated using the Hillshade tool with four azimuth angles (0°, 45°, 90°, 135°) to enhance microrelief expression.

Lineament extraction was conducted using the LINE MODULE in PCI Geomatica 2018 (Figure 9).

After semi-automatic detection, features were filtered and interpreted to identify structural alignments. Dominant orientations included SE-NW, E-W, and N-S. The highest density of lineaments corresponded with slope breaks, morphological edges, and ring-shaped fault structures in the valley center.

These linear features coincide spatially with GPR-detected loosening zones, reinforcing the role of tectonic controls in karst formation, groundwater flow, and geohazard development in the study area.

6. Correlation of morphometric characteristics of relief, lineaments and zones of decompression in the Saura Valley

The integration of DEM data, lineament interpretation, and GRR profiles revealed distinct spatial patterns in the development of karst processes in the Saura Valley. Analysis of morphometric parameters (slope, aspect, curvature, and vertical dissection) showed that the loosening zones detected by the GPR are confined to areas with significant slopes ($>15\text{-}20^0$) and local slope breaks, where high values of vertical dissection (up to 22.6 m/m^2) are recorded.

These conditions promote the development of gravitational processes such as landslides and scree – that increase the permeability of the rock formations. Analysis of slope aspect revealed that the main loosening zones are concentrated on northern, north-eastern, and eastern slopes. Comparison with the relief curvature map showed that most anomalies are associated with areas of positive curvature (convex ridges and slopes) and zones of abrupt transitions between convex and concave forms, where tensile stresses accumulate and subsurface faults are exposed. Lineament analysis of the DEM using PCI Geomatica revealed several dominant lineament systems (SE-NW, E-W, and N-S) and a high lineament density in the eastern and southern sectors of the valley. The most pronounced GPR anomalies spatially coincide with the intersection points of these lineaments, confirming the structural control of karstification and the development of decompression zones along tectonic faults. The mapped lineaments and decompaction zones exhibit a strong spatial correlation, particularly along the framing cliffs and within the central depressed portion of the valley.

This configuration indicates the presence of tectonic faults and zones of enhanced fracturing, which facilitate moisture infiltration and localized leaching of carbonate rocks. The combined analysis of relief morphometric parameters and GPR data confirms that karst processes in the Saura Valley are structural-tectonic in origin and develop predominantly along zones of tectonic weakening. The results highlight the importance of considering tectonic conditions and morphometric indicators when predicting geodynamic hazardous areas.

The integrated application of UAV surveys, GNSS measurements, morphometric analysis, and GPR has proven effective for identifying potentially unstable karst zones in arid environments and has enabled a comprehensive reinterpretation of karst morphodynamics in the Saura Valley (Chen, 2020; Plan, 2021). The spatial correlation between GPR-detected zones of soil loosening, lineament concentrations, and morphometric indicators such as steep slopes (>25°), extreme curvature values, and vertical dissection exceeding 22.6 m/mI confirms the structurally controlled nature of karst development in the study area. Notably, these zones coincide with ring-shaped fault structures and are concentrated in the eastern and southern sectors, where SE–NW and E–W lineament orientations dominate. The intersection of lineaments appears to intensify gravitational instability, suggesting a heightened risk of ground collapse.

These findings emphasize the role of tectonic lineaments as preferential pathways for groundwater flow and zones of rock weakening, thereby supporting previous studies indicating that fault systems serve as principal controls on karstification in arid carbonate terrains (Nechayev & Strokova, 2023). The observed alignment of structural elements with geophysical anomalies provides a strong basis for interpreting the spatial evolution of karst in the region.

Morphometric analysis further supports this conclusion, indicating that karst features are concentrated within fractured Neogene limestones with high porosity and permeability. This lithological setting, typical of arid-zone karst, facilitates both surface dissolution and subsurface cavity formation. The presence of sinkholes, collapsed niches, and open fractures points to a polyphase genesis likely linked to neotectonic uplift and episodic humid intervals during the Late Neogene-Quaternary, consistent with broader geomorphological reconstructions.

The UAV-based data acquisition, processed via Structure-from-Motion (SfM) techniques in Agisoft Metashape, proved effective for producing detailed digital surface models, while GNSS data from the SOUTH Galaxy G9 system ensured precise spatial referencing. The integration of these datasets significantly improved the reliability of surface–subsurface correlation. Ground-penetrating radar surveys using the Zond Aero LF system identified three distinct decompression zones at depths up to 20 meters. The heterogeneous geological environment marked by abrupt lithological transitions and structural discontinuities enhanced geophysical contrasts and facilitated the detection of features indicative of potential subsidence or void formation. These results underscore the value of GPR as a non-invasive tool for karst hazard assessment in inaccessible or infrastructurally limited areas. Importantly, these geophysical anomalies require verification through borehole drilling and further correlation with geotechnical and hydrogeological data. Such investigations are critical for assessing surface stability and validating subsurface models.

In conclusion, this study demonstrates the effectiveness of a multidisciplinary geospatial approach for characterizing karst systems in arid regions. Continued application of high-precision technologies will advance our understanding of the spatial and temporal dynamics of karst evolution in the Mangystau region.

Beyond scientific relevance, the results have practical implications for geohazard monitoring, slope stability assessment, and environmental management in vulnerable karst landscapes.

CONCLUSION

For the first time, a comprehensive approach to studying the karst terrain of the Saura valley has been implemented, based on the use of high-precision data collection and analysis methods such as UAVs, GNSS, geophysical surveys, and GIS. This has enabled the acquisition of a detailed understanding of the morphometry, structure, and formation factors of karst features under the arid climate conditions of Mangystau.

The development of karst in the studied region is driven by complex interactions among geological-structural, lithological, hydrogeological, and climatic factors, with the morphology of the terrain playing a key role in the localization and development direction of karstogenesis. Tectonic dissection and fracturing of carbonate rocks facilitate the infiltration of atmospheric precipitation and underground circulation, thereby activating dissolution processes. Favorable structural and geological conditions in the region support the development of modern karst processes even under arid climate conditions.

The results obtained not only clarify the understanding of the karst morphology of the Saura valley but also open up prospects for further research of similar natural formations in the region.

Research conducted using an integrated approach allows not only to characterize karst terrains in detail, but also to develop measures to reduce anthropogenic impact. Intensive tourism and active infrastructure development can accelerate karst processes and increase the likelihood of emergencies. Created orthophotomaps and digital terrain models allow the identification of potentially dangerous areas enables timely implementation of preventive measures. The introduction of an early warning system, regular monitoring, and adaptive management helps to reduce risks to the population and the natural environment, while preserving the recreational potential of the studied territory.

The presented methodology can be recommended for assessing slope stability, geomorphological hazards, and predicting karst processes in similar environmental conditions.

Abbreviations

UAV	Unmanned aerial vehicle
GPR	Ground Penetrating Radar
DEM	Digital elevation model
GNSS	Global Navigation Satellite System

Author Contributions: Conceptualization, A. B. and R. T.; methodology, A. B. and Zh. Sh.; validation, A. B. and R. T.; formal analysis, A. B. and Zh. Sh.; investigation, A. B. and Yu. L.; resources, Zh. Sh.; writing–original draft preparation, A. B., Yu. L. and Zh. Sh.; writing–review and editing, A. B., R. T.; visualization, A. B. and Yu. L.; supervision, R. T.; project administration, R. T.; funding acquisition, R. T. All authors have read and agreed to the published version of the manuscript.

Funding: This research was funded by Committee of Science of the Ministry of Science and Higher Education of the Republic of Kazakhstan, grant №AP23490612 “Comprehensive assessment of karst origin tourist objects of Mangystau region for development of recommendations and measures for their conservation and safe use”. The APC was funded by the same grant.

Institutional Review Board Statement:

Informed Consent Statement: Not applicable.

Data Availability Statement: The data used for the present work include proprietary data, which cannot be shared in their original format.

Acknowledgements: The authors would like to thank the research workers of “Geotourism and geomorphology” laboratory of “Institute of Geography and Water security” JSC, that helped us during our surveys in Mangystau region and especially Rakhimov F. and Taskynbayev A. for the assistance in conducting geophysical research and data processing.

Conflicts of Interest: The authors declare no conflict of interest.

REFERENCES

Abdelouhed, F., Ahmed, A., Abdellah, A., & Mohammed, I. (2021). Lineament mapping in the Ikniouen area (Eastern Anti-Atlas, Morocco) using Landsat-8 Oli and SRTM data. *Remote Sensing Applications: Society and Environment*, V. 23, 100606. https://doi.org/10.1016/j.rsase.2021.100606.

Abdeltawab, S. (2013). Karst limestone foundation geotechnical problems, detection and treatment: Case studies from Egypt and Saudi Arabia. *International Journal of Scientific & Engineering Research*, V. 4(5), 376-387.

Al-Rawabdeh, A., He F., Moussa A., El-Sheimy N., & Habib, A. (2016). Using an unmanned aerial vehicle-based digital imaging system to derive a 3D point cloud for landslide scarp recognition. *Remote Sens.*, 8(2), 95. https://doi.org/10.3390/rs8020095

Aigner, S., Hauser, & Schmitt, A. (2023). Pattern-based detection of sinkholes in arid zones using open-source satellite imagery: A case study in Kazakhstan in 2023. *Sensors* 2025, 25, 798. https://doi.org/10.3390/s25030798

Akziz, D., Nemer, Z., Colavitto, B., Guettouche, M. S., Goumrasa, A., & Belaroui, A. (2022). Geomorphic analysis and quaternary neotectonic deformation in the eastern Babors chain, Bejaia, Algeria. *Journal of African Earth Sciences*, 185, 104387. https://doi.org/10.10.1016/j.jafrearsci.2021.104387

Aliyev, A. A. (2015). *Karstovye protsessy i formy relyefa Zapadnogo Kazakhstana [Karst Processes and Landforms of Western Kazakhstan]*. – Geomorphology, No. 1, 45–52 (in Russian).

Batayneh, A. T., Abueladas, A. A., & Moumani, K. A. (2002). Use of ground-penetrating radar for assessment of potential sinkhole conditions: an example from Ghor al Haditha area, Jordan. *Environmental Geology*, V. 41(8), 977-983. https://doi.org/10.1007/s00254-001-0477-8

Billi, A., De Filippis, L., Poncia, P. P., Sella, P., & Faccenna, C. (2016). Hidden sinkholes and karst cavities in the travertine plateau of a highly-populated geothermal seismic territory (Tivoli, central Italy). *Geomorphology*, V. 255, 63-80. https://doi.org/10.1016/j.geomorph.2015.12.011

Chen, H., Jiang, G., & Yuan, D. (2020). Karst development and evolution in arid regions: insights from remote sensing and geophysical investigation. *Geomorphology*, 367, 107299.

Chikishev, A. G. (1973). *Peshchery na territorii SSSR [Caves of the USSR territory] / Editor E. M. Murzayev. Series: The present and future of the Earth and humanity*. M.: Nauka, 137. (in Russian).

Diercks, M. L., Grützner, C., Welte, J., & Ustaszewski, K. (2023). Challenges of geomorphologic analysis of active tectonics in a slowly deforming karst landscape (W Slovenia and NE Italy). *Geomorphology*, 440, Article 108894. https://doi.org/10.1016/j.geomorph.2023.108894

Ebraheem, M. O., & Ibrahim, H. A. (2019). Detection of karst features using ground-penetrating radar: a case study from the western limestone plateau, Assiut, Egypt. *Environ Earth Sci* 78, 563. https://doi.org/10.1007/s12665-019-8572-x;

El Hadani, D. (1997). *Télédétection et Système d'information Géographique Pour La Gestion et La Recherche de l'eau [Remote Sensing and Geographic Information System for Water Management and Research]*. IAHS Publications-Series of Proceedings and Reports-Intern Assoc Hydrological Sciences 242., Wallingford [Oxfordshire]: IAHS, 1981: 197–204. (in French)

El Hameedy, M. A., Mabrouk, W.M., Dahroug, S., & Metwally, A.M. (2023). Detection of karst features and associated geohazard using ground penetrating radar and 2D electrical resistivity imaging; case study from Sannur protectorate, Egypt. *Contributions to Geophysics and Geodesy*, 53(3), 167–190. https://doi.org/10.31577/congeo.2023.53.3.1

Faure, S. (2001). *Analyse des linéaments géophysiques en relation avec les minéralisations en or et métaux de base de l'Abitibi [Analysis of geophysical lineaments in relation to gold and base metal mineralization in Abitibi]*. Rapport, Projet CONSOREM 2000-03A, 26 p. (in French)

Ford, D. C., & Williams, P. (2007). *Karst Hydrogeology and Geomorphology*. – Chichester: John Wiley & Sons, 562 p.

Frumkin, A., Ezersky, M., Al-Zoubi, A., Akkawi, E., & Abueladas, A. R. (2011). The Dead Sea sinkhole hazard: Geophysical assessment of salt dissolution and collapse. *Geomorphology*, 134(1-2), 102-117. http://dx.doi.org/10.1016/j.geomorph.2011.04.023

Funk, B., Flores-Orozco, A., & Steiner, M. (2024). Possibilities and limitations of cave detection with ERT. *Geomorphology*, 462, 109332. https://doi.org/10.1016/j.geomorph.2024.109332

Garova, E., Chadromtsev, B., Pedanov, A., Grebennikov, P., Iltuganov, I., Lobanov, P., & Fuchs, S. (2025). A general methodological framework for hazard assessment in remote mountain areas combining geomorphological mapping with UAV survey. *Journal of Mountain Science*, 22(3), 763-775. https://doi.org/10.1007/s11629-024-9096-8

Ghadimi, M., Zangenehtabar, S., Malekian, A. & Kiani, M. (2022). Groundwater vulnerability assessment in a karst aquifer: a case study of western Iran. *Int. J. Environ. Sci. Technol.* 19(8), 7503-7516. https://doi.org/10.1007/s13762-022-03956-9

Goldscheider, N., & Drew, D. (2007). *Methods in Karst Hydrogeology*. London: Taylor & Francis, 264 p.

Gutiérrez, F., Parise, M., De Waele, J., & Jourde, H. (2014). A review on natural and human-induced geohazards and impacts in karst. *Earth-Science Reviews*, 138, p. 61–88. https://doi.org/10.1016/j.earscirev.2014.08.002

Gutiérrez, F., Galve, J. P., Lucha, P., Castañeda, C., Bonachea, J., & Guerrero, J. (2011). Integrating geomorphological mapping, trenching, InSAR and GPR for the identification and characterization of sinkholes: A review and application in the mantled evaporite karst of the Ebro Valley (NE Spain). *Geomorphology*, 134(1–2), 144–156. https://doi.org/10.1016/j.geomorph.2011.01.018

Gvozdetczky, N. A. (1972). *Problemy izuchenya karsta i praktika [Problems of karst study and practice]*. M: Mysl., 392 (in Russian).

Hobbs, W. H. (1912). *Earth Features and Their Meaning: An Introduction to Geology for the Student and the General Reader*, Macmillan, 506 p.

Iskakov, S. D. (2019). *Unikal'nyye prirodnyye ob"yekty Mangistauskoy oblasti i ikh znacheniye dlya ustoychivogo razvitiya regiona [Unique natural objects of the Mangystau region and their significance for the sustainable development of the region]*. *Scientific Journal "Geography and Natural Resources"*, 40(4), 58–63. (in Russian).

Jarzyna, A., Bąbel, M., Czajkowska, M., & Ługowski, D. (2024). Morphometry and morphology of the gypsum tumuli from the Sorbas karst region, SE Spain. *Geomorphology*, 465, 109403. https://doi.org/10.1016/j.geomorph.2024.109403

Kleiner, Y. M. (1970). *Karst i neftegazonosnost' Zapadnogo Kazakhstana [Karst and oil and gas potential of Western Kazakhstan]*. – Alma-Ata: Nauka, 84 (in Russian).

Kulbayeva, G. A. (2018). *Geologicheskoe stroenie i karstovye obrazovaniya Mangistauskogo plato [Geological structure and karst formations of the Mangystau plateau]*. Bulletin of KazNU. Geological Series, No. 3(72), 22–28 (in Russian).

Kuznetsov, Y. Y. (1965). *Karst Ustyurta i Mangyshlaka [Karst of Ustyurt and Mangyshlak]*. M: Nauka, 187 (in Russian).

La Salandra, M., Roseto, R., Mele, D., Dellino, P., & Capolongo, D. (2022). Probabilistic hydro-geomorphological hazard assessment based on UAV-derived high-resolution topographic data: The case of Basento river (Southern Italy). *Science of The Total Environment*, 842, 156736.

Lacina, C. (1996). *Interprétation Structurale Des Linéaments Par Traitement d'image Satellitaire: Cas Des Sousprovinces d'Abitibi et d'Opatica (Québec) [Structural Interpretation of Lineaments by Satellite Image Processing: Case of the Abitibi and Opatica Subprovinces (Quebec)]*. Memory Presented in Faculty of Humanities, University of Sherbrooke Quebec, Canada (in French)

Large, A. R. G., & Heritage, G. L. (2009). Laser Scanning – Evolution of the Discipline. In: Heritage G.L., and Large A.R.G, editors. Laser Scanning for the Environmental Sciences, Wiley-Blackwell, West Sussex, UK. 1-20. https://doi.:10.1002/9781444311952

Le Mesnil, M., Moussa, R., Charlier, J. B., & Caballero, Y. (2021). Impact of karst areas on runoff generation, lateral flow and interbasin groundwater flow at the storm-event timescale. *Hydrology and Earth System Sciences*, 25(3), 1259–1282. https://doi.org/10.5194/hess-25-1259-2021

Masoud, A. A., & Koike, K. (2006). Arid Land Salinization Detected by Remotely-Sensed Landcover Changes: A Case Study in the Siwa Region, NW Egypt. *Journal of Arid Environments*, 66 (1). Elsevier: 151–167.

Moslemi, H., Karimi, H., Birtwisle, A., & Ghiyasi, M. (2023). Detection of karstic conduits using deep ground-penetrating radar (DGPR) in cretaceous limestone (case study: Bakan plain, Fars province, South Iran). *Carbonates Evaporites* 38(3), 58. https://doi.org/10.1007/s13146-023-00878-6)

Nechayev, D. A., & Strokova, L. A. (2023). *Otsenka karstovo-suffozionnoy opasnosti territorii trassy nefteprovoda "Chayanda–VSTO" [Assessment of karst-suffosion hazard of the territory along the Chayanda-VSTO oil pipeline route]*. *Proceedings of Tomsk Polytechnic University. Engineering of geological resources*, 334, 7, 78–92. (in Russian).

Öztürk, M. Z., Poyraz, M., Duman, H., & Taşoğlu, E. (2025). A geospatial approach to understanding sinkhole formation in Akgöl Wetland, Türkiye. *Environmental Earth Sciences*, 84(8), 209. https://doi.org/10.1007/s12665-025-12225-0

Plan, L., Hausmann, H., & Keuschnig, M. (2021). Modern karst processes and hazards in high-alpine and arid environments. *Geomorphology*, 387, 107783

Potapova, G. M., & Bekkuliyeva, A. A. (2010a). Karst Regionalization Map. Atlas of the Mangystau Region, Almaty, p. 160.

Potapova, G. M., & Bekkuliyeva, A. A. (2010b). Karst processes of the Mangystau Peninsula and their zoning // Second Announcement & Call for Papers. The Caspian Region: Environmental Consequences of the Climate Change, Moscow, 173–176.

Pour, A. B., Hashim, M., & van Genderen, J. (2013). Detection of hydrothermal alteration zones in a tropical region using satellite remote sensing data: Bau goldfield, Sarawak, Malaysia. *Ore Geology Reviews*, 54, Elsevier, 181–196. https://doi.org/10.1016/j.oregeorev.2013.03.010

Pozachenyuk, Y. A., & Petlyukova, Y. A. (2016). *GIS-analiz morfometricheskikh pokazateley rel'yefa tsentral'nogo predgor'ya Glavnoy gryady Krymskikh gor dlya tseley landshaftnogo planirovaniya [GIS analysis of morphometric indicators of the relief of the central foothills of the Main range of the Crimean Mountains for the purposes of landscape planning]. Journal Scientific Notes of the V.I. Vernadsky Crimean Federal University, Geography, Geology*, 2(68), 95-111 (in Russian).

Prodanov, B., Kotsev, I., Lambev, T., Dimitrov, L., Bekova, R., & Dechev, D. (2019). Drone-based geomorphological and landscape mapping of Bolata Cove, Bulgarian coast. In Sustainable Development and Innovations in Marine Technologies 592-596. *CRC Press.*

Pueyo-Anchuela, O., Casas-Sainz, A. M., Soriano, M. A., & Pocoví-Juan, A. (2010). A geophysical survey routine for the detection of doline areas in the surroundings of Zaragoza (NE Spain). *Engineering Geology*, 114(3-4), 382-396. http://dx.doi.org/10.1016/j.enggeo.2010.05.015

Reynolds, J. M. (1997). An Introduction to Applied and Environmental Geophysics. – Wiley, New York, 796

Rohaendi, N., Sukiyah, E., Muslim, D., & Cipta, A. (2021). Geo-tourism land suitability analysis of Citatah karst area in Bandung basin using spatial multi criteria evaluation (SMCE). *GeoJournal of Tourism and Geosites*, 39(4spl), 1346–1353. https://doi.org/10.30892/gtg.394spl04-777

Samuel, C., Magagi, R., Yergeau, M., & Sylla, D. (2010). An Integrated Approach to Hydro-Geological Lineament Mapping of a Semi-Arid Region of West Africa Using Radarsat-1 and GIS. *Remote Sensing of Environment*, 114 (9). Elsevier: 1863–1875.

Sharapkhanova Zh.M., Lyy Y.F., & Yegemberdiyeva K.B. (2024). Assessment and mapping of the mudflow phenomena intensity in Charyn state national natural park. *Geojournal of Tourism and Geosites*, 55(3), 1148–1155. https://doi.org/10.30892/gtg.55315-1287

Siart, C., Bubenzer, O., & Eitel, B. (2009). Combining digital elevation data (SRTM/ASTER), high resolution satellite imagery (Quickbird) and GIS for geomorphological mapping: A multi-component case study on Mediterranean karst in Central Crete. *Geomorphology*, 112(1–2), 106–121. https://doi.org/10.1016/j.geomorph.2009.05.010

Spiridonov, A. I. (1970). *Osnovy obshchey metodiki polevykh geomorfologicheskikh issledovaniy i geomorfologicheskogo kartografirovaniya [Fundamentals of the general methodology of field geomorphological research and geomorphological mapping]*. – Moscow: Higher School, Russian Federation (in Russian).

Strokova, L. A., Ezhkova, A. V., & Leonova, A. V. (2020). *Primeneniye lineamentnogo analiza dlya otsenki karstoopasnosti pri proyektirovanii magistral'nogo gazoprovoda v yuzhnoy Yakutii [Application of lineament analysis to assess the karst hazard in the design of the main gas pipeline in south Yakutia]*. Bulletin of the Tomsk Polytechnic University, Geo Assets Engineering, 331 (11), 117-126. https://doi.org/10.18799/24131830/2020/11/2891 (in Russian).

Takasu, T., & Yasuda, A. (2009). Development of the low-cost RTK-GPS receiver with an open source program package RTKLIB // Int. Symp. on GPS/GNSS. – Jeju, Korea: Int. Conv. Cent. http://gpspp.sakura.ne.jp/paper2005/isgps_2009_rtklib_ revA.pdf

Tallini, M., Gasbarri, D., Ranalli, D., & Scozzafava, M. (2006). Investigating epikarst using lowfrequency GPR: example from the Gran Sasso range Central Italy. *Bulletin of Engineering Geology & Environment*, 65, 435–443

Theilen-Willige, B., Malek, H., Charif, A., El Bchari, F., & Chaïbi, M. (2014). Remote Sensing and GIS Contribution to the Investigation of Karst Landscapes in NW-Morocco. *Geosciences*, 4(2), 50–72. https://doi.org/10.3390/geosciences4020050

Tjoelker, A. R., Baraër, M., Valence, E., Charonnat, B., Masse-Dufresne, J., Mark, B. G., & McKenzie, J. M. (2024). Drone-Based Ground-Penetrating Radar with Manual Transects for Improved Field Surveys of Buried Ice. *Remote Sensing*, 16(13), 2461. https://doi.org/10.3390/rs16132461

Torsuyev, N. P. (1980). *Geographicheskiye aspecty izuchenya ravninnogo karsta [Geographical aspects of the study of plain karst]*/ N.P. Torsuyev, S. A. Levin. – Kazan, p. 183. (in Russian).

Tsirélson, B. S., & Popov, V. A. (2010). *Karta «Geologiya» [Map "Geology"]. Scale 1:1,500,000. Atlas of Mangystau Region*, Almaty, p. 20 (in Russian).

Vassilakis, E., & Konsolaki, A. (2022). Quantification of cave geomorphological characteristics based on multi source point cloud data interoperability. *Zeitschrift Für Geomorphologie*, 63(2–3), 265–277. https://doi.org/10.1127/zfg/2021/0708

Vlasov, G. I. (1988). *Karst v zasushlivykh rayonakh SSSR [Karst in arid regions of the USSR]*. – M: Nedra, p. 230, (in Russian).

Westoby, M. J., Brasington, J., Glasser, N. F., Hambrey, M. J., & Reynolds, J. M. (2012). 'Structure-from-Motion' photogrammetry: a low-cost, effective tool for geoscience applications. *Geomorphology*, 179, 300–314. https://doi.org/10.1016/j.geomorph.2012.08.021.

Yalcin, C. (2025). Comprehensive Examination of Gypsum Deposits and Identification of Karstic Cavities Utilizing Ground Penetrating Radar in the Bala Region (Ankara-Türkiye). *Iranian Journal of Earth Sciences.* https://doi.org/10.57647/j.ijes.2025.16972

Youssef, A. M., Al-Harbi, H. M., Gutiérrez, F., Zabramwi, Y. A., Bulkhi, A. B., Zahrani, S. A., & El-Haddad, B. A. (2016). Natural and human-induced sinkhole hazards in Saudi Arabia: distribution, investigation, causes and impacts. *Hydrogeol J* 24(3), 625–644. https://doi.org/10.1007/s10040-015-1336-0

Zhang, W., Jiang, T., & Han, M. (2010). *Digital camera calibration method based on PhotoModeler //3rd Int*. Congress on Image and Signal Processing, IEEE, 1235–1238. https://doi.org/10.1109/CISP.2010.5647253

Article history: Received: 09.07.2025 Revised: 12.11.2025 Accepted: 08.12.2025 Available online: 31.12.2025